Reentry produced by small-scale heterogeneities in a discrete model of cardiac tissue

Sergio Alonso and Markus Bär

Physikalisch-Technische Bundesanstalt, Abbestrasse 2-12, 10587 Berlin, Germany

E-mail: sergio.alonso@ptb.de

Abstract. Reentries are reexcitations of cardiac tissue after the passing of an excitation wave which can cause dangerous arrhythmias like tachycardia or life-threatening heart failures like fibrillation. The heart is formed by a network of cells connected by gap junctions. Under ischemic conditions some of the cells loss their connections and the excitability is decreased. We consider a circular region with a fraction of heterogeneities surrounded by homogeneous tissue, where the heterogeneities represent blocked gap junctions. This heterogeneous region is characterized by the fraction of blocked gap junctions (resp. missing connections) or by the fraction of gaps in the tissue. Such region is shown to act as a source of new waves which reenter into the tissue and reexcitate the whole heart. We study the statistics of such reentries in two dimensions and relate the probability of reentry to the percolation threshold of the fraction of heterogeneities for different networks topologies.

1. Introduction

Cardiac tissue is an example of an excitable media where electrical travelling waves propagate. The propagation of such electrical signal through the tissue synchronizes the contraction of all the fibers of the heart. The electrical signal corresponds to a pulse-like wave of membrane action potential, which is around 5 cm width, that propagates at high speed, 0.5 m/s [1]. The general propagation properties of such waves are similar to chemical waves in the Belousov-Zhabotinsky reaction or the oxidation of CO on catalytic surfaces [2]. In excitable media waves may break up giving rise to spiral waves of excitation [3]. In cardiac tissue such spiral waves have been experimentally observed [4] and are associated to tachycardia [1]. The presence of multiple spirals and spatiotemporally chaotic dynamics is related to ventricular fibrillation [5].

The electrical wave is generated by the depolarization of the cellular membrane of the myocytes. The depolarization permits the influx of different types of ions and in particular of calcium which induces the contraction of the cardiac fibers. Myocytes are electrically active cells 100-120 μm long and 10-20 μm wide and are coupled by gap junctions. Such junctions permit the propagation of the membrane depolarization to the neighbouring cells and maintain wave propagation. Research on modeling of the electrical activity of the myocytes has produced models with a large number of equations whose details depend on the type of animal or the level of detail in the description, for a survey of physiological models see for example [6, 7].

The large spatial scale of the electrical propagating waves in comparison with the size of the myocytes, has usually permitted the use of homogenization theories to generate continuous models of action potential propagation in cardiac tissue [3]. However, during the last years more detailed models of cardiac tissue including the individual cells have appeared in two [8] and

three [9] dimensional tissue. It permits also the inclusion of other types of cells like fibroblast [10] or non-conducting tissue originated by fibrosis [11].

The inclusion of heterogeneities at the cellular level affect the dynamics of the macroscopic waves. The velocity, for example, decreases with the number of included heterogeneities [12, 13, 14] because the connectivity between the cells is reduced and the communication is slower [15]. The decrease of the velocity implies a reduction of the excitability of the medium and it may preclude spiral breakup in two-dimensional tissue [12] or induce negative filament tension [16, 17] in three dimensional slabs. Cardiac propagation can be perturbed by a so-called reentry of the excitation, e.g. by spontaneous formation of spirals due to ectopic beats. The accumulation of the heterogeneities in a particular region of the system may generate reentries [18, 19] due to the formation of a source-sink mismatch [20, 21]. On the other hand, heterogeneities can be also employed as virtual electrodes to generate a large number of new waves to suppress fibrillatory electrical activity [22, 23].

Here, we consider the generation of reentries by a heterogeneous circular region and we study the different types of reentries found in the numerical simulations changing the topology of the discrete network of connected cells. For all the cases we find similar relation between proximity of the heterogeneity fraction to the critical value for percolation [24] and the probability to obtain reentrant activity [19]. We perform a detailed analysis for different topology of the networks.

The paper is organized as follows: in Section 2 we include the three levels of modelization considered and the types of topologies employed. In Section 3 we show the main results obtained from more than 20000 simulations. The paper ends with the main conclusions from the analysis of the numerical results.

2. Model

2.1. Continuous tissue model

The propagation of the action potential is described by the cable equation [3]. Such equation relates the variation of the membrane potential (V) with the total current due to the ion channels across the membrane (I), and the conduction of potential along the cell membrane. The cable equation reads:

$$\frac{\partial V}{\partial t} = -I + \nabla \cdot (D \nabla V), \tag{1}$$

where $D = 0.001\ cm^2/ms$ is the effective diffusion coefficient of the action potential, which is proportional to the conductivity tensor.

The total current I is a sum of different types of ion currents $I = \sum_i I_i$. The number and complexity of these currents determines the particular ionic model employed [6]. Here we use a simplified model, which consists in only three ion currents [5, 25]:

$$\frac{\partial V}{\partial t} = -(I_{fi} + I_{so} + I_{si}) + \nabla \cdot (D \nabla V), \tag{2}$$

where the currents do not exactly correspond to an explicit ion channel, but are controlled by parameters which can be fitted to particular experimental measurements or to more complex models. The ionic currents read:

$$\begin{aligned} I_{fi} &= \frac{-vp(V - V_c)(1 - V)}{\tau_d}, \\ I_{so} &= \frac{V(1-p)}{\tau_o} + \frac{p}{\tau_r}, \\ I_{si} &= \frac{-w(1 + tanh(k(V - V_c^{si})))}{2\tau_{si}}, \end{aligned} \tag{3}$$

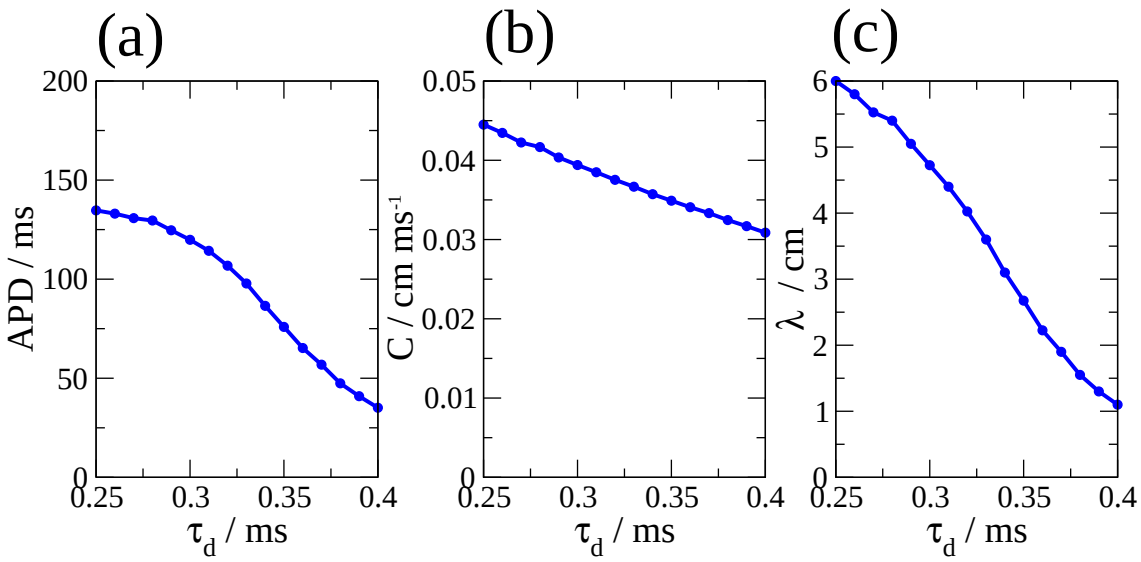

Figure 1. Dependence of the propagation parameters in the medium excitability. Monotonous decrease of the APD (a), linear decrease of the wave velocity (b) and decrease of the wave size (c) on the model parameter τ_d.

corresponding, respectively, to the fast inward, slow outward and slow inward currents. These currents are controlled by the gating variables v and w. The evolution of such gate variables depends on the action potential:

$$\begin{aligned} \frac{\partial v}{\partial t} &= \frac{(1-p)(1-v)}{\tau_v^-(V)} - \frac{pv}{\tau_v^+}, \\ \frac{\partial w}{\partial t} &= \frac{(1-p)(1-w)}{\tau_w^-} - \frac{pw}{\tau_w^+}; \end{aligned} \tag{4}$$

where $\tau_v^-(V) = (1-q)\tau_{v1}^- + q\tau_{v2}^-$ with $p = \theta(V - V_c)$ and $q = \theta(V - V_v)$, where $\theta(x)$ is the Heaviside step function.

During our study we vary the parameter τ_d keeping constant the value of the rest of parameters: $\tau_v^+ = 3.33ms$, $\tau_{v1}^- = 19.6ms$, $\tau_{v2}^- = 1000ms$, $\tau_w^+ = 667ms$, $\tau_w^- = 11ms$, $\tau_o = 8.3ms$, $\tau_r = 50ms$, $\tau_{si} = 45ms$, $k = 10$, $V_c^{si} = 0.85$, $V_c = 0.13$ and $V_v = 0.055$, for more details see [5]. For $\tau_d = 0.25$ the propagating waves obtained in the numerical integration of eq.(2) together with eq.(3, 4) reproduce the main properties of the waves obtained by the numerical integration of the Beeler-Reuter model [26]

We employ finite differences for the spatial discretization ($\Delta x = 250\ \mu m$) and a second order Runge-Kutta method for the temporal integration of the equations ($\Delta t = 0.15\ ms$) for the numerical integration of eqs.(2-4).

The combination of the nonlinealities controlling the total current I with the transport of the action potential determined by the parameter D, produces the stationary propagation of a wave through the cardiac tissue which coordinates the contraction of the heart. Waves with free ends produce the formation of spiral waves. Spirals are related with reentry in cardiac tissue which leads to tachycardia.

The action potential duration (APD) decreases with the parameter τ_d, see Fig. 1. Thus, waves are smaller and slower for larger values of τ_d, meaning that excitability decreases with this parameter. As the value of τ_d is increased, the APD decreases, see Fig.1(a), the velocity

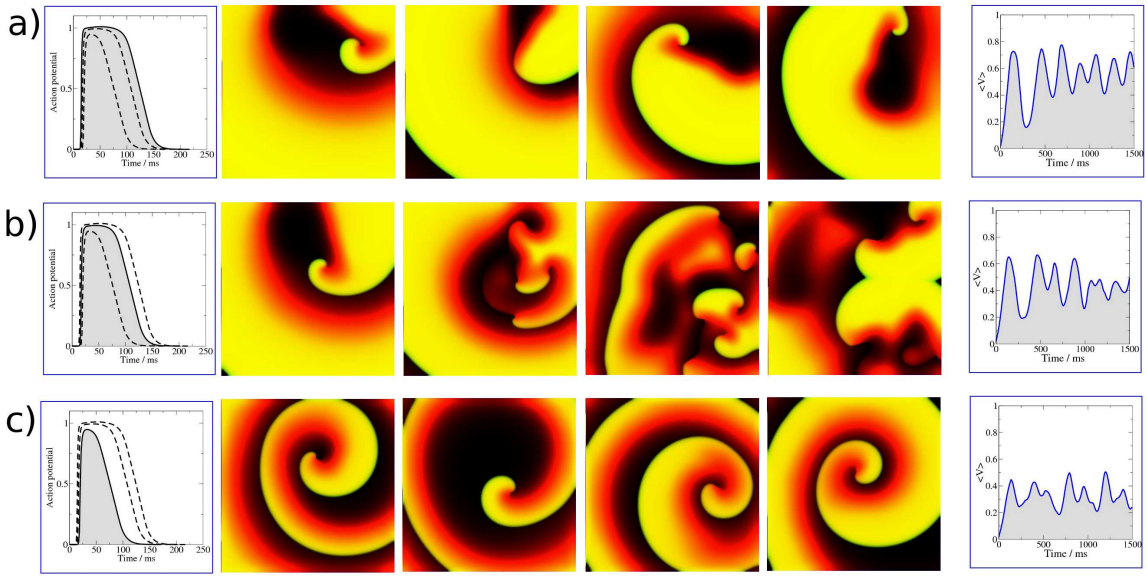

Figure 2. Dynamics of two-dimensional wave propagation in a homogeneous continuous model for three different values of $\tau_d =: 0.25ms$ (a), $0.30ms$ (b) and $0.35ms$ (c). For each value of $\tau_d =$ we show the evolution of the action potential of an individual cell (left panel), four snapshots corresponds to times 480 ms, 660 ms, 960 ms and 1200 ms (middle panel), and the average of the action potential ($< V >$) in the whole domain (right panel). Square grid 10×10 cm^2 with $\Delta t = 0.15$ ms and $\Delta x = 0.025$ cm.

of the traveling waves (C) decreases practically linearly, see Fig.1(b), and the wave size (λ), defined by the product of these two quantities ($\lambda = C \cdot APD$), also decreases, see Fig.1(c).

In Fig. 2 we show the spiral wave dynamics for three different values of τ_d. For each case, we show first the action potential for a single point, second four snapshots showing the evolution of a spiral wave and finally the integration of the value of V for the whole area $< V >= A^{-1} \int V dA$. For $\tau_d = 0.25$ and $\tau_d = 0.30$ large action potentials are obtained and the interaction of the waves of the spiral with the refractory tail of the previous wave produces complex behaviours and even spiral breakup as it is shown in Fig. 2(b). The development of the spiral breakup depends on the initial condition and the size of the system, it is also obtained under some conditions for $\tau_d = 0.25$. Waves for large values of τ_d behaves similar as pulses in FitzHugh-Nagumo models [27] and zones with weak excitability are reached. Further increase of τ_d brings the system to the non-excitable region and precludes the propagation of waves [5].

2.2. Discrete network of cells

In contrast with the continuous description of the cardiac tissue, here we consider a two-dimensional network of cells connected by gap junctions. The excitability of the cells are governed by the ion equations described above. The electrical connectivity between the cells is assumed to be at first neighbours and it corresponds to diffusion in the continuous limit. An equivalent equation to eq.(2) can be calculated for each cell i as follow:

$$\frac{\partial V_i}{\partial t} = -(I_{fi} + I_{so} + I_{si}) + \xi \sum_{j}^{N} (V_j - V_i), \tag{5}$$

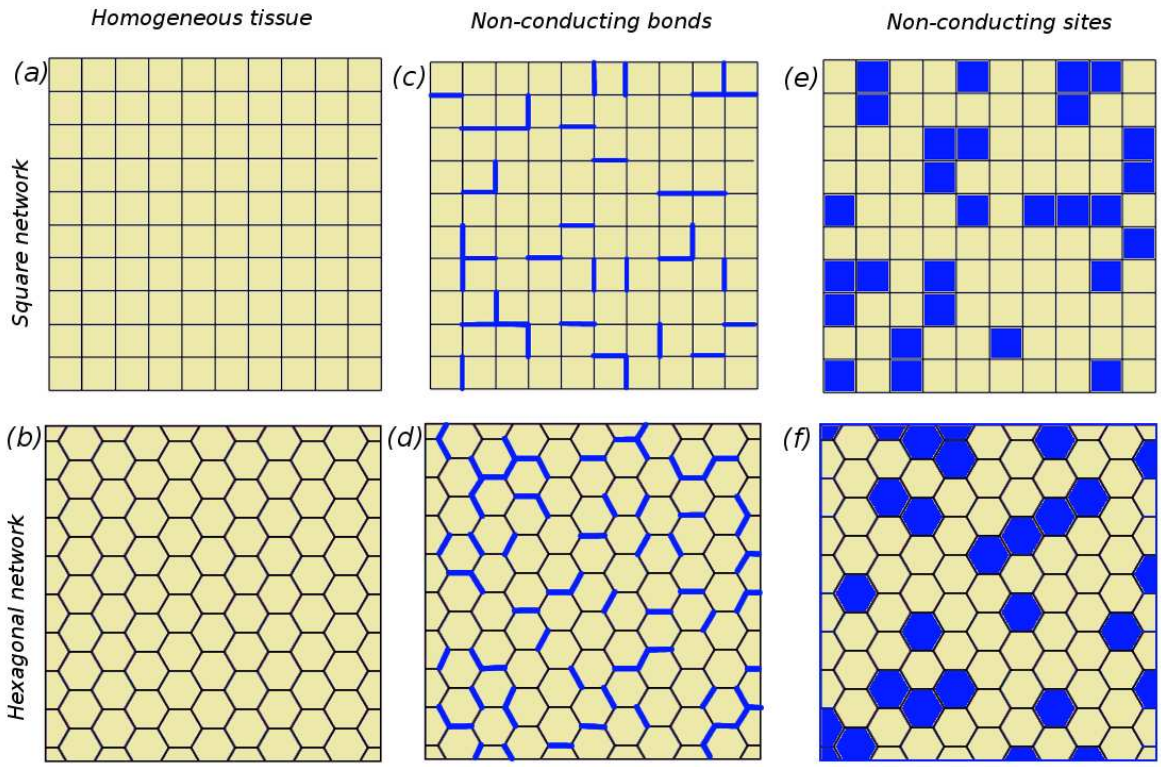

Figure 3. Types of networks: Homogeneous Square (a), homogeneous hexagonal (b), heterogeneous square with non-conducting bonds (c), heterogeneous hexagonal with non-conducting bonds (d), heterogeneous square with non-conducting sites (e), heterogeneous hexagonal with non-conducting sites (f).

where N is the number of first neighbours: four for a square network, see Fig.3(a), and six for a cubic network, see Fig.3(b). The parameter ξ is chosen in order to recover the homogeneous limit of eq.(2) and reads $\xi = D/\Delta x^2$; where $\Delta x = 0.01\ cm$ is the distance between cells centers or, i. e., size of the cells.

2.3. Heterogeneous discrete network of cells

Inactive gap junctions, inert tissue among the cardiac cells or the presence of unexcitable cells, e.g. fibroblast, in the tissue breaks the continuous and homogeneous propagation of action potential through the cardiac tissue, and the resulting waves are rough and noisy. We model this disruption in the propagation by the introduction of random heterogeneities in the network of cells using eq.(5) together with a connectivity parameter η_{ij}:

$$\frac{\partial V_i}{\partial t} = -(I_{fi} + I_{so} + I_{si}) + \xi \sum_{j}^{N} \eta_{ij}(V_j - V_i), \tag{6}$$

if the connectivity parameter $\eta_{ij} = 1$ for all i and j we recover the homogeneous discrete network limit of eq.(5). We consider here than the value of η_{ij} can take only two values: $\eta_{ij} = 1$ for normal connections between two cells and $\eta_{ij} = 0$ for abnormal connections. These abnormal connections are randomly scattered in the tissue, thus, we do not consider any correlation.

We study two types of heterogeneities:

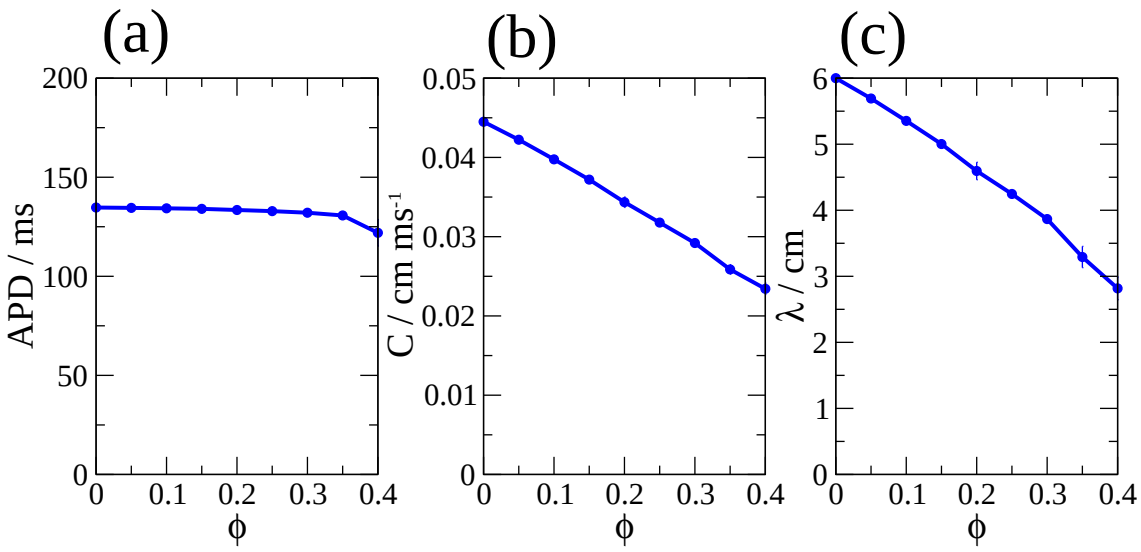

Figure 4. Dependence of the propagation parameters in the fraction of heterogeneities ϕ. Independence of the APD (a), linear decrease of the wave velocity (b) and decrease of the wave size (c) on the parameter ϕ.

- *Non-conducting bonds.* The connection between two cells (i and j) is removed ($\eta_{ij} = 0$) with certain probability ϕ which is independent of the connectivity with the rest of first neighbours, see Fig. 3(c,d).
- *Non-conducting sites.* For a certain probability ϕ a cell (i) is abnormally connected with all the first neighbours ($\eta_{ij} = 0, \forall\ j$), see Fig. 3(e,f).

These two interpretations gives rise to different types of discrete networks of cells with different topological properties.

The introduction in the medium of a randomly distributed fraction of heterogeneities affects the dynamics of the propagating waves. As example we first consider the case of non-conducting bonds in a square network. The propagation of waves in the medium depends on the fraction of heterogeneities ϕ. As the heterogeneities do not modify the ion currents, the APD in each cell remains independent on the fraction ϕ, see Fig.4(a). The velocity of wave propagation, however, clearly depends on ϕ, and it decreases for increasing ϕ, see Fig.4(b). The decrease of the velocity produces an equivalent decrease of the wave size, see Fig.4(c).

The increase of the fraction of the heterogeneities produce the appearance of clusters of isolated regions surrounded by removed links or cells. For a particular fraction ϕ_c the network percolates, i.e. a cluster of the system size separates the whole medium in two disconnected parts [24]. The critical fraction ϕ_c for non-conducting bonds and sites is different and gives rise to two different percolation thresholds. Above the percolation threshold of the cell network wave propagation is not more possible. Close to such value, the velocity rapidly decrease to zero [14] and the wave size approaches the size of the heterogeneities, inducing wave breakup, and giving rise to complex dynamics [19].

2.4. Localized heterogeneous region inside a discrete network of cells

In the numerical simulations we divide the system in two parts, see Fig.5 for a sketch of the system:

- *Damaged region:* a circular heterogeneous region corresponding to a damaged area of the tissue. The heterogeneities are introduced with a fraction ϕ in a circular region of the tissue.

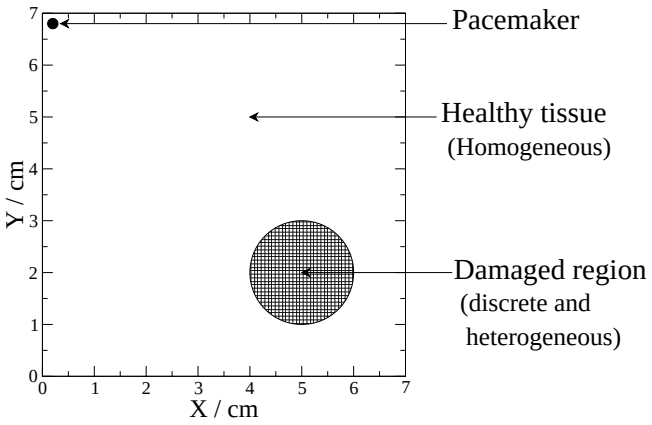

Figure 5. Sketch of the system employed for the numerical simulations. Waves are initially generated at the pacemaker and propagate normally in the homogeneous tissue till the wave interact with the damaged region, which is highly heterogeneous and where reentries are formed.

This region represents a damaged area of the tissue where the parameter τ_d is also modified by the decrease of the excitability.

- *Healthy tissue:* a normal homogeneous region corresponding to the healthy tissue. The propagation of the action potential recovers the standard properties.

We evaluate the interaction between the wave propagating in an homogeneous region of the tissue with the damaged region with a fraction of heterogeneities. An excitation wave of action potential is initially induced in one corner of the two-dimensional system, mimicking a pacemaker, see Fig.5. The excitation propagates through the medium till it interacts with the circular region. Depending on the relation between ϕ and ϕ_c (percolation threshold) three behaviours are observed:

- *For low fraction ($\phi << \phi_c$):* the wave propagates inside the damaged region. The wave deforms and propagates inside slower than outside, however, wave propagation is stable.
- *For large fraction ($\phi >> \phi_c$):* the wave does not enter in the damaged region and the it propagates around this region.
- *For intermediate fraction ($\phi \sim \phi_c$):* the wave propagates in the circular region, however the propagation inside is highly irregular. The different possibilities obtained from the numerical simulations under such condition are discussed in the next section.

3. Results

3.1. Types of reentries

As already stated in the previous section, wave propagation is irregular for $\phi \sim \phi_c$. The most frequent behaviour corresponding to the interaction between the wave and the damaged heterogeneous region for $\phi \sim \phi_c$ is a transient propagation of the wave inside the damaged region that rapidly disappears. There are, however, other dynamics when the propagation inside the heterogeneous region persists. We classify the new behaviours into three different groups:

- *Sustained reentry:* The pieces of waves inside the circular region survive after the wave pass and repeatedly propagate to the boundary of the circle giving rise to reentry. An example of such behaviour is shown in Fig.6. The moving pieces produce a new wave which excites the whole medium again Fig.6(a). These pieces produce a pacing of the homogeneous region and if the reentry path inside the circular region is fast enough, it can even break the waves

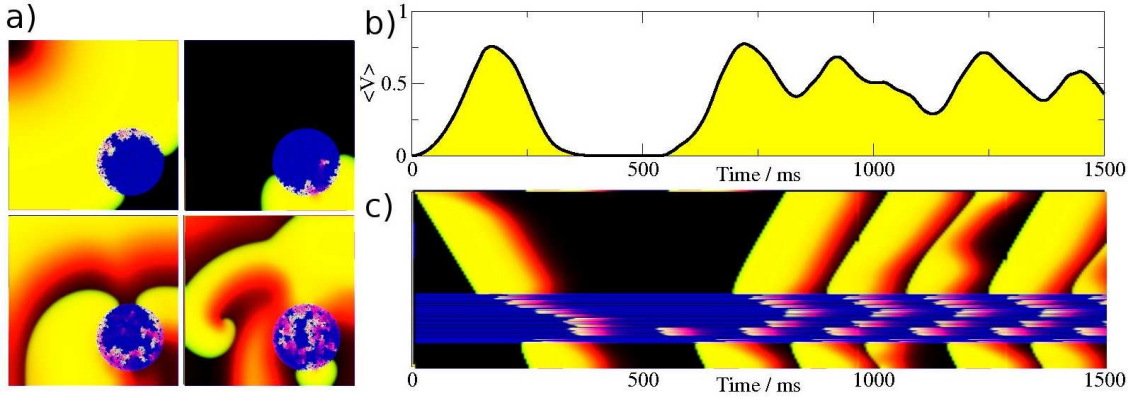

Figure 6. Sustained reentry induced in a damaged region of the tissue. (a) Four snapshots of the evolution of the reentry for times: 184 ms, 598 ms, 1002 ms and 1398 ms. (b) Evolution of the global spatial average of the action potential showing the activity of the tissue. (c) Spatio-temporal dynamics from a diagonal cut of the system which crosses the damaged area and illustrates the activity inside and outside the damaged region. Parameter values: Radius of the circular inhomogeneity: 1.4 cm; inside the damaged area $\phi = 0.49$ and $\tau_d = 0.35ms$; and square network 7×7 cm^2.

by the interaction with the refractory tail of the previous wave as shown in Fig.6(a), and produce the formation of spiral waves. The evolution of the total excitation of the medium ($< V >$) is also plotted and shows the intense excitation of the system from the reentry, see Fig.6(b). Finally, the spatio-temporal plot shown in Fig.6(c) permit the observation of the interaction among the waves induced by the circular region. When the path inside the heterogeneous region is large the pacing is slow and it produces a stable pacemaker of new waves.

- *Non-sustained reentry:* The first wave generated by the previous mechanism interacts with the wave inside the circular region and eliminate the activity, see Fig.7. A single event is produced which basically reset the whole heterogeneous system again. Different cases with two or three reentries and the final reset to the rest state have been also observed in the numerical simulations.
- *Residual patterns:* If the excitability of the medium inside the circular region is very low in comparison to the outside medium, the wave may not be able to reenter into the homogeneous highly excitable medium. Then the pieces of waves are restricted to propagate inside the heterogeneous region. An example of such dynamics is shown in Fig.8. The average activity ($< V >$) of the medium is not zero but small, see Fig.8(b), and there is a periodic dynamics restricted to the circular region produced by the continuous repetition of the reentry path inside the heterogeneous system, see Fig.8(c).

The three types of dynamics have been observed in the numerical simulations. They can appear in different random realizations under exactly the same conditions and they can appear simultaneously, for instance a non-sustained reentry can finish in a residual pattern. As we show below, the probability of reentry depends not only on ϕ but also on the size, excitability and network topology of the circular heterogeneous region.

3.2. Relation of the reentry probability with the percolation threshold

We study the probability of appearance of the different dynamical patterns by increasing systematically the fraction of non-conducting bonds ϕ in a square network. We increase ϕ

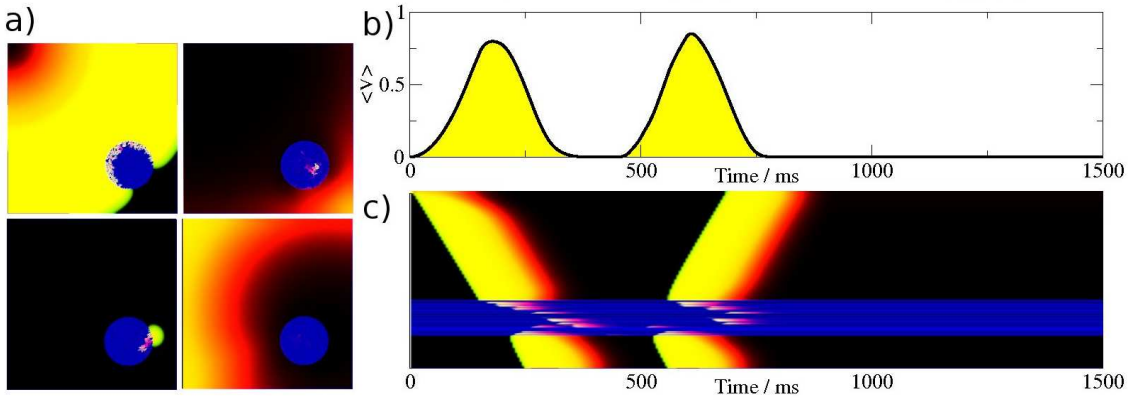

Figure 7. Non-sustained reentry induced in a damaged region of the tissue. (a) Four snapshots of the evolution of the reentry for times: 184 ms, 345 ms, 469 ms and 717 ms. (b) Evolution of the global spatial average of the action potential showing the activity of the tissue. (c) Spatio-temporal dynamics from a diagonal cut of the system which crosses the damaged area and illustrates the activity inside and outside the damaged region. Parameter values: Radius of the circular inhomogeneity: 1 cm; inside the damaged area $\phi = 0.495$ and $\tau_d = 0.35ms$; and square network 7×7 cm^2.

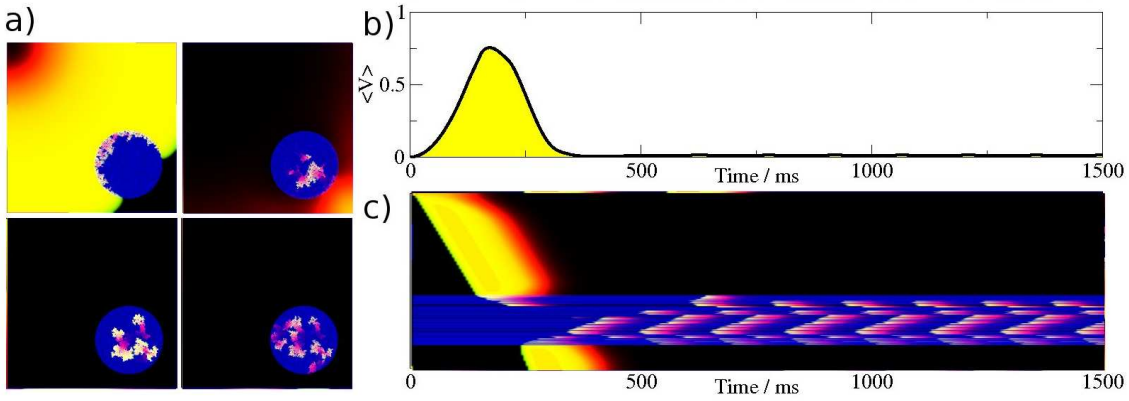

Figure 8. Residual reentry induced in a damaged region of the tissue. (a) Four snapshots of the evolution of the reentry for times: 184 ms, 349 ms, 483 ms and 763 ms. (b) Evolution of the global spatial average of the action potential showing the activity of the tissue. (c) Spatio-temporal dynamics from a diagonal cut of the system which crosses the damaged area and illustrates the activity inside and outside the damaged region. Parameter values: Radius of the circular inhomogeneity: 1.4 cm; inside the damaged area $\phi = 0.49$ and $\tau_d = 0.35ms$; and square network 7×7 cm^2.

on small steps ($\Delta\phi = 0.005$) and for each value of ϕ we perform 100 realizations of the same numerical experiment with different random distribution of the heterogeneities.

The dependence of the probability of the three types of reentries on ϕ is shown in Fig.9. At low and large values of ϕ reentries do not appear. For a window of intermediate values ($\phi \sim \phi_c$) the three types of reentries are observed. The higher probability of reentry is obtained at $\phi = 0.48$ while the percolation threshold for the square network with non-conducting bonds is $\phi_c = 0.5$.

The most common reentry is the sustained reentry (74%) while non-sustained (13%) and the

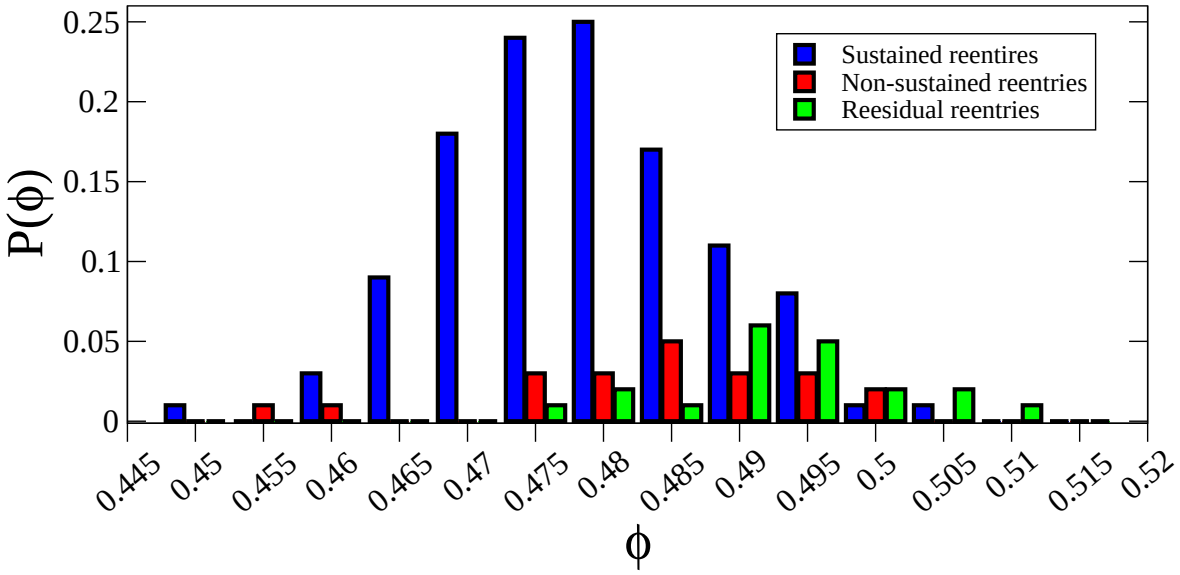

Figure 9. Probability of the different types of reentries produced by a circular heterogeneous region for different values of ϕ. Three types of interactions are observed: sustained reentry, non-sustained reentry and residual patterns. The radius of the inhomogeneity is kept constant $R = 1.4\ cm$. The parameter τ_d is spatially inhomogeneous: $\tau_d = 0.25ms$ outside and $\tau_d = 0.35ms$ inside the damaged region. A total of 100 realizations have been done for each value of ϕ.

residual patterns (13%) are less frequent. The relative probability of the non-sustained reentries and residual patterns is higher for large values of ϕ. A possible reason for such effect is that at high values of ϕ the propagation inside the damaged region is slower. Such reduction of the velocity is equivalent to an effective reduction of the excitability. The difference of excitability between inside and outside the region is, therefore, larger. A gap in excitability hinders the exit of the wave, as it is known for generic excitable media.

3.3. Dependence on the size of the damaged region

We also study the effect of the size of the damaged region. If the region is small the entrance of the wave in the damaged region rapidly excites the active cells. A possible reentrance into the homogeneous healthy region would rapidly interact with the posterior part of the initial wave, which hinder the appearance of the reentry. Given a value of τ_d there is a minimal size of the circular area which can induce reentries.

We define the total number of reentries for all the possible heterogeneity fraction ($0 < \phi < 1$) as control parameter: $U = \sum_i NP(\phi_i)$ where $NP(\phi_i)$ is the number of reentries observed after N=100 realizations with ϕ_i. As already note in the previous subsection we increase the fraction of heterogeneities in a discrete way: $\phi_i = i\Delta\phi$. In Fig. 10(a) the dependence of this quantity U on the radius of the circular damaged region is shown. As the radius increases the number of reentries grows.

The relative fractions of the different types of reentries change also with the size of the damaged region. For low radius the distribution is centered around the percolation threshold. However, for larger radius the center of the distribution moves to lower values of ϕ [19]. This displacement produces that the majority of reentries appear at higher excitability (low values of ϕ) and the case of sustained reentry is the most probable. For smaller regions the distribution of the three types of reentries is more homogeneous, for example for $R_0 = 0.8cm$ we observe

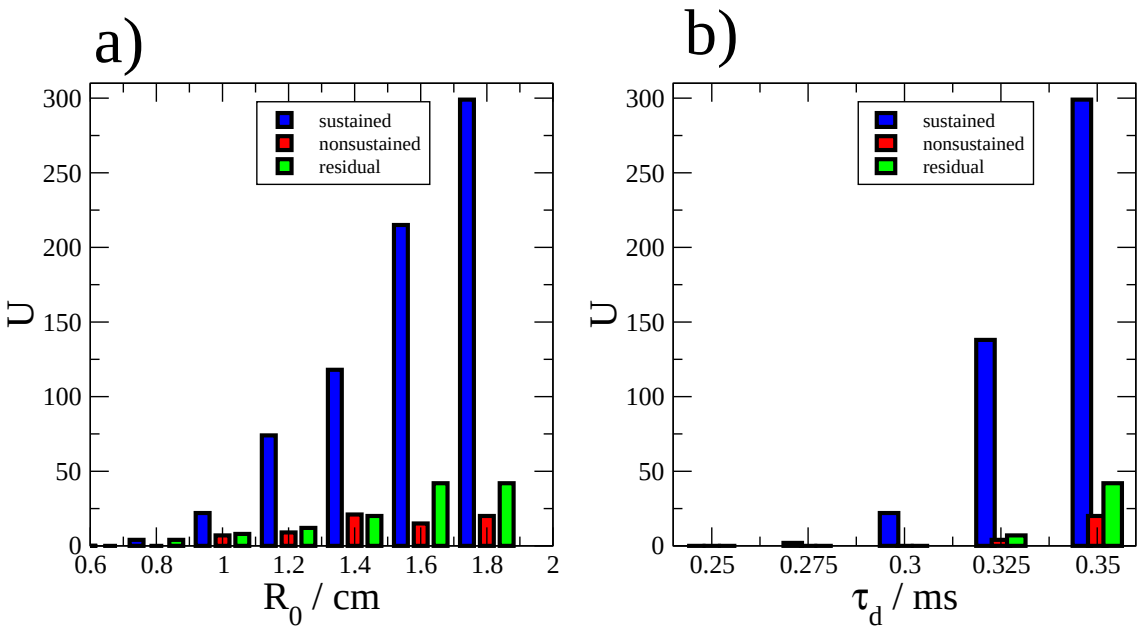

Figure 10. a) Total reentry probability for the three different types of reentry for different radius keeping $\tau_d = 0.35ms$ (a) and for different values of τ_d keeping $R_0 = 1.8cm$ (b). Parameter τ_d outside the damaged region is kept $\tau_d = 0.25ms$.

50% sustained reentries and 50% of residual patterns, in comparison with the results shown in Fig. 9.

3.4. Dependence on the excitability of the damaged region

We perform simulations under different excitability conditions. We change the value of the parameter τ_d inside the damaged region. The numerical results show a clear dependence of the probability on the value of this parameter, see Fig. 10(b). For standard conditions of the model ($\tau_d = 0.25$) reentries are not observed in the numerical simulations. The increase of the parameter τ_d decreases the velocity and APD of the waves inside the damaged region and permits the appearance of the reentries, see Fig. 10(b). The probability of reentry increases with τ_d.

The distribution of the three types of reentries depends also on the excitability of the medium, see Fig. 10(b). For larger excitability, i.e small τ_d, the probability of reentry is small and all the cases are associated to sustained reentries. For smaller excitability, i.e large τ_d, the other two types of reentries also are observed. The relative probability of non-sustained and residual reentries increases with τ_d.

3.5. Probability of reentry on different topologies of the networks of cells

The previous results are obtained by changing the fraction of non-conducting bonds in a square grid. Next, we consider other types of topologies and heterogeneities, keeping the size of the damaged region and the excitability inside this region. We consider square or hexagonal grids with non-conducting bonds or sites, see Fig.3.

In Fig. 11 the dependence of the probability of the three types of reentries on the fraction ϕ is plotted for different topologies keeping the values of the parameters. The interaction of a travelling wave with the heterogeneous region in a square or in a hexagonal grid produces the onset of reentries for fraction values close to the particular percolation threshold of the

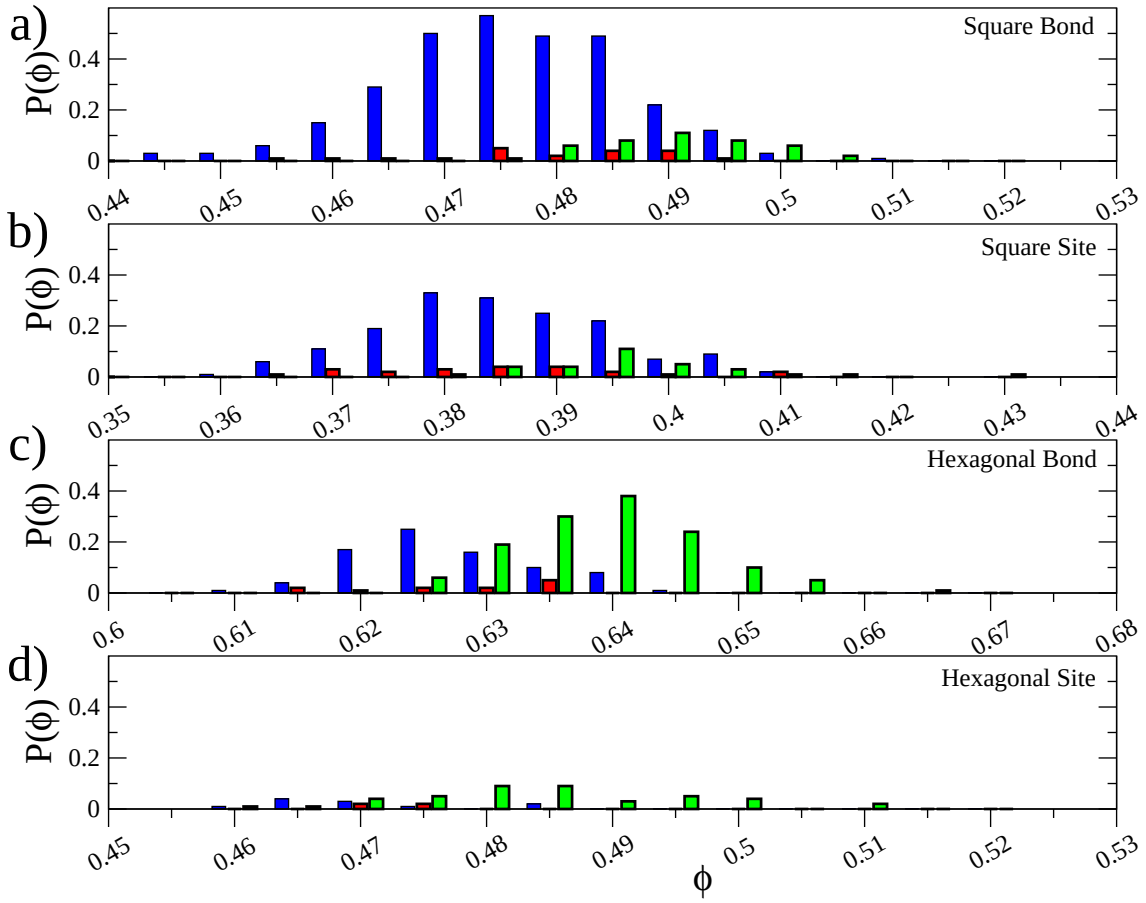

Figure 11. Probability of the different types of reentries produced by a circular heterogeneous region for different values of ϕ for different topologies and heterogeneity types: a) Square network with site heterogeneities, b) Square network with site heterogeneities, c) Hexagonal network with bond heterogeneities, and d) Hexagonal network with site heterogeneities. The radius of the inhomogeneity is kept constant $R = 1.8\ cm$. The parameter τ_d is spatially inhomogeneous: $\tau_d = 0.25$ outside and $\tau_d = 0.35$ inside the damaged region.

Table 1. Distribution of the different types of reentries corresponding to Fig. 11

Topology	Threshold	Total	Sustained	Non-sustained	Residual
Square Bond	0.5	361	299 (83%)	20 (5%)	42 (12%)
Square Site	0.41	220	167 (76%)	22 (10%)	31 (15%)
Hexagonal Bond	0.65	227	82 (36%)	12 (5%)	133 (59%)
Hexagonal Site	0.5	58	11 (19%)	4 (7%)	43 (74%)

corresponding network. In this figure the distribution of the type of reentries as function of ϕ is also plotted. For all grid topologies, while sustained reentries appear typically for small values of ϕ, residual patterns dominates at large fractions.

Although for the four cases the probability of reentry is related with the percolation threshold,

the results shown in Fig. 11 indicate a dependence of the relative probability of the reentries on the topology:

- *Square vs. hexagonal:* Square grids produces higher probability of reentry than hexagonal grids under the same conditions. Furthermore, the distribution of the reentries is different, whole in square grids around 80% of reentries correspond to sustained, in hexagonal grids the major part of reentries (59% and 74%, see Table 1) are residual.
- *Bond vs. Sites:* While the distributions of the different types of reentries does not depend on the type of heterogeneity, site or bond, there is a decrease of the total number of reentries in the case of site heterogeneities in comparison with bond heterogeneities, see Table 1 and Fig. 11.

4. Conclusions

We employ an heterogeneous discrete model of cardiac tissue to numerically study the reentry produced by a damaged region (modelled as an heterogeneous discrete system) inside the healthy tissue (homogeneous). Following, we list the main conclusions after the realization of more than 20000 numerical simulations:

- Heterogeneous tissue may produce reentry if the fraction of non-conducting heterogeneities is close to the percolation threshold of the network.
- The reentries are classified in three main types: sustained, non-sustained and residual, depending in their capability of survive and to leave from the damaged region where are generated to the healthy area.
- The probability of reentry depends on the size and excitability of the damaged region.
- The probability of reentry depends on the type of heterogeneities, reentries produced by non-conducting bonds are more frequent than by non-conducting sites.
- The type of the network changes the predominant type of the reentry. While for square networks sustained reentry are more common, for hexagonal networks residual reentries are more frequent.

These conclusions are relevant for the understanding of anatomical reentry in cardiac tissue. Extensions of the employed model have to consider the three-dimensional structure of the tissue, which changes the topological properties, and more concrete models of cellular networks in real cardiac tissue.

An additional biological example of heterogeneous excitable media is myocyte cell cultures. In such case heterogeneities play a crucial role in the pattern formation processes [28, 29], because the lack of orientation which myocytes do present in tissue.

In summary, the use of well established concepts in physics like percolation threshold in discrete networks can improve the general understanding of reentries in cardiac tissue which may lead to dangerous arrhythmia.

Acknowledgements

We acknowledge financial support from the German Science Foundation DFG within the framework of SFB 910 "Control of self-organizing nonlinear systems".

References

[1] D. P. Zipes, and J. Jalife, *Cardiac Electrophysiology: From Cell to Bedside* (Philadelphia, PA: Saunders, 2004).
[2] *Chemical Waves and Patterns*, edited by R. Kapral and K. Showalter (Kluwer, Dordrecht, 1994).
[3] J. P. Keener, and J. Sneyd, *Mathematical Physiology* (New York: Springer, 1998).
[4] Davidenko J M, Pertsov A M, Salomonz R, Baxter W, and Jalife J, 1992 *Nature* **335** 349

[5] Fenton F H, Cherry E M, Hastings H M, and Evans S J, 2002 *Chaos* **12** 852
[6] Clayton R H, Bernus O, Cherry E M, Dierckx H, Fenton F H, Mirabella L, Panfilov A V, Sachse F B, Seemann G, and Zhang H, 2011 *Prog. Bio. Phys. Mol. Biol.* **104** 22-48
[7] Fenton F H, and Cherry E M, 2008 *Scholarpedia* **3** 1868
[8] Gouvea de Barros B, Sachetto Oliveira R, Meira W, Lobosco M, and Weber dos Santos R, 2012 *Comp. Math. Meth. Med.* 824569
[9] Stinstra J G, MacLeod R, and Henriquez C S, 2010 *Ann Biomed Eng* **38** 1390-1414.
[10] Xie Y, Garfinkel A, Camelliti P, Kohl P, Weiss J N, and Qu Z, 2009 *Am J Physiol Heart Circ Physiol* **297** H775-H784
[11] Qu Z, Karagueuzian H S, Garfinkel A, and Weiss J N, 2004 *Am. J. Physiol. Heart Circ. Physiol.* **286** H1310
[12] Panfilov A V, 2002 *Phys. Rev. Lett.* **88** 118101
[13] Ten Tusscher K H W J, and Panfilov A V, 2007 *Europace* **9**, vi38
[14] Alonso S, Kapral R, and Bär M, 2009 *Phys. Rev. Lett.* **102** 238302
[15] Rohr S, 2004 *Cardiovas. Res.* **62** 309-322
[16] Alonso S, Bär M, and Panfilov A V, 2011 *Chaos* **21** 013118
[17] Alonso S, Bär M, and Panfilov A V, 2013 *Bull. Math. Biol.* **75** 1351-1376
[18] Cherry E M, Ehrlich J R, Nattel S, and Fenton F H, *Heart Rhythm* **4** 1553-1562 (2007).
[19] Alonso S, and Bär M, 2013 *Phys. Rev. Lett.* **110** 158101
[20] Kleber A G, and Rudy Y, 2004 *Physiol. Rev.* **84** 431-488
[21] Kinoshita S, Iwamoto M, Tateishi K, Suematsu N J, and Ueyama D, 2013 *Phys. Rev. E* **87** 062815
[22] Pumir A, Nikolski V, Hörning M, Isomura A, Agladze K, Yoshikawa K, Gilmour R, Bodenschatz E, and Krinsky V, 2007 *Phys. Rev. Lett.* **99** 208101
[23] Luther S, Fenton F H, Kornreich B G, Squires A, Bittihn P, Hornung D, Zabel M, Flanders J, Gladuli A, Campoy L, Cherry E M, Luther G, Hasenfuss G, Krinsky V, Pumir A, Gilmour R F Jr and Bodenschatz E, 2011 *Nature* **475** 235
[24] Torquato S, *Random Heterogeneous Materials* (Springer, New York, 2002).
[25] Fenton F H, and Karma A, 1998 *Chaos* **8** 22
[26] Beeler, G W, Reuter H, 1977 *J. Physiol* **268** 177-210
[27] FitzHugh R, 1961 *Biophys. J.* **1** 445
[28] Bub G, Shrier A, and Glass L, 2002 *Phys. Rev. Lett.* **88** 058101
[29] Steinberg B E, Glass L, Shrier A, and Bub G, 2006 *Phil. Trans. R. Soc. A* **364** 1299-1311